



Cite this: *RSC Adv.*, 2020, **10**, 8002

The inhibition of H1N1 influenza induced apoptosis by sodium selenite through ROS-mediated signaling pathways

Guifang Gong,^{†,a} Yinghua Li,^{†,b} Kunyan He,^a Qiumei Yang,^a Min Guo,^b Tiantian Xu,^b Changbing Wang,^b Mingqi Zhao,^b Yi Chen,^b Miaomiao Du,^a Bingyuan Li,^a Yanqing Huang^{*a} and Bing Zhu^{ID, *b}

The high variability of influenza viruses has made it more difficult for people to cope with influenza. When antigen transformation occurs, even new influenza without preventive vaccines may be produced, which poses a great threat to human health. Selenium is an essential trace element in humans and mammals, and has many biological activities. It has attracted people's research interest in recent years. In this study, MDCK cells were used as a model to observe the effect of sodium selenite on H1N1 influenza virus. Our research showed that sodium selenite (Na_2SeO_3) has an anti-influenza H1N1 virus effect, and the anti-viral effect of sodium selenite was further demonstrated by caspase-3, AKT, MAPK and p53 signaling pathways. The investigations of the mechanism revealed that the sodium selenite could block H1N1 influenza from infecting MDCK cells through inhibiting the production of ROS. The results demonstrate that selenium supplementation may provide a feasible approach to inhibit the infection of H1N1 influenza virus.

Received 15th November 2019

Accepted 15th February 2020

DOI: 10.1039/c9ra09524a

rsc.li/rsc-advances

1 Introduction

Influenza viruses cause seasonal epidemics of human diseases as well as large-scale morbidity and high mortality.^{1–3} The classification of influenza A virus is based on different combinations of hemagglutinin (HA) and neuraminidase (NA) which were the protein on the surface of the virus.⁴ In the past century, there were three influenza A viruses: H1N1, H2N2 and H3N2 leading to human pandemics.⁵ Nowadays, antiviral treatment relies mainly on drugs that target the virus.⁶ Neuraminidase inhibitors inhibit the release of budding virus particles by host cells, primarily by binding to the active site of neuraminidase. The M2 inhibitor achieves an antiviral effect by blocking the ion channel activity of the influenza A virus M2 protein during the viral phase.⁷ Continuous antigenic drift and antigenic translation of viral surface glycoproteins make it a major factor in the unpredictable effects of influenza vaccines.^{8–10} Vaccine protection is not effective enough to provide reliable protection for humans.^{11–13} At present, due to the rising resistance of influenza virus to existing anti-influenza drugs, we urgently need to find new antiviral drugs.^{14–16}

As an essential trace element, selenium participates in many biological activities of the human body, including the intensification, differentiation and proliferation of immune cells.^{17–19} Inorganic selenium has four forms of existence in nature: selenate, selenite, elemental Se and selenide.^{20–22} These forms are converted by the biological system into selenoamino acids selenocysteine and selenomethionine, a more bioavailable organic form.²³ The prognosis of some infectious diseases has been confirmed to be related to the body's selenium content.²⁴ In some studies, selenium has been shown to have antiviral effects, but the exact mechanism is not clear.^{25–28} It is an important component of glutathione peroxidase (GSH-Px) and active center, acting as a free radical scavenger to protect cells from oxidative stress.^{29–31}

Free radicals in the human body can damage cells, tissues and organs, affect health, and shorten life expectancy.^{32–35} Antioxidants are “free agent scavengers” and have a catalytic effect on the treatment and prevention of many diseases.^{36,37} Studies have shown that more ROS are detected in host cells after viral infection, which is related to the degree of viral infection.^{38–40} Therefore, the ROS level can indirectly reflect the level of virus replication and speculate that virus replication and intracellular redox system linked.^{41–43} Several apoptosis related protein, antioxidant proteins and oxidative damage inhibitors have been reported by Leung *et al.*^{44–46} Flavokawain A, a novel Chaconne from Kava extract induces apoptosis in bladder cancer cells by Zi *et al.*⁴⁷ The apoptotic effect of nanosilver is mediated by a ROS and JNK dependent

^aDepartment of Obstetrics Gynecology, Guangzhou Women and Children's Medical Center, Guangzhou Medical University, No. 402 Renminzhong Road Yuexiu District, Guangzhou, 510120, China. E-mail: YanqingHuang2018@hotmail.com

^bCenter Laboratory, Guangzhou Women and Children's Medical Center, Guangzhou Medical University, Guangzhou, 510120, China. E-mail: zhubing2016@hotmail.com

† Guifang Gong and Yinghua Li contributed equally to the work.



mechanism involving the mitochondrial pathway in NIH3T3 cells by Hsin *et al.*⁴⁸ Similarly, the goal of preventing the replication of influenza A virus can be achieved by inhibiting activity and inhibiting the production of oxygen.⁴⁹ The oxidative stress pathway is very important for targeted treatment.⁵⁰ Therefore, this study ascertains how sodium selenite will antagonize H1N1 influenza virus induced MDCK cells apoptosis through ROS-mediated signaling pathways.

2 Experimental

2.1 Materials

MDCK cells were purchased from American Type Culture Collection (ATCC® CCL-34™). H1N1 influenza virus was provided by Virus laboratory, Guangzhou institute of pediatrics, Guangzhou Women and Children's Medical Center, Guangzhou Medical University. Dulbecco's modified Eagle's medium (DMEM), trypsin-EDTA (0.25%) (phenol red) and fetal bovine serum (FBS) were purchased from Gibco. TPCK Trypsin was purchased from Thermo Scientific. Caspase-3, PARP, p53 and AKT antibody were obtained from Cell Signaling Technology. 2',7'-Dichlorofluorescein diacetate (DCFH-DA) were obtained from Sigma. Cell Counting Kit was obtained from Beyotime Biotechnology. Milli-Q water was purification from Millipore in all experiments.

2.2 Preparation of Na₂SeO₃ stock solution

The preparation of sodium selenite solution was as follow: 0.017 g of sodium selenite solid powder was put into 100 mL of distilled water. The concentration of stock solution was 1 mM, the stock solution was put in 4 °C refrigerator for use.

2.3 Determination of the TCID₅₀ of H1N1

Cells were cultured in 96-well plate at a density of 8×10^4 cells per well and incubated for 24 hours. Then removed the original medium, washed the plates twice with PBS, the virus stock was placed in an EP tube and diluted with a medium containing 2 $\mu\text{g mL}^{-1}$ TPCK trypsin-free serum at a ratio of 10 times, 10^{-1} , 10^{-2} , 10^{-3} , 10^{-4} , 10^{-5} , 10^{-6} , 10^{-7} , 10^{-8} , 10^{-9} respectively, and each dilution was inoculated with a tandem A total of 8 wells, each inoculated with 100 μL . The control group was also set up in a column and cultured in 36.5 °C and 5% CO₂ incubator. After 2 hours of adsorption, removed the medium, washed the plates twice with PBS, then 200 μL of serum-free medium containing 2 $\mu\text{g mL}^{-1}$ TPCK trypsin was added and placed in incubator. 50% cell culture infectious dose (TCID₅₀) was then calculated according to the Reed-Muench calculation method.

2.4 Cell culture and cell viability by cell counting kit-8 assay B (CCK-8)

MDCK cells were seeded in 96-well culture plates at a density of 4×10^4 cells per well for 24 h, there were four groups as follow: normal cell control group, single drug control group, virus control group and virus plus drug treatment group. After

the virus was incubated for 2 hours, all the groups were changed medium and washed with PBS twice. Serum-free medium 200 μL was added to the normal cell control group and the virus control group, and the serum-free medium containing 1 μM of sodium selenite 200 μL was added to the drug-only control group and the virus plus drug-treated group. Then these four groups were placed in the incubator. Observed cytopathic conditions for 72 h, added 10 μL of CCK-8 solution to each well, and the mixture was incubated for 2 hours. Cell viability was measured at 450 nm using a microplate spectrophotometer.

2.5 Activation of caspase-3

Caspase-3 activity was measured according to the methods described as previously described.⁵¹ Cell lysates, detection buffer and specific caspase substrates Ac-DEVD-pNA (2 mM) were added into a 96-well plate for 2 h at 37 °C. The activation of caspase-3 was measured through the conversion of pNA, which was measured by 405 nm absorbance using a microplate reader.

2.6 Measurement of reactive oxygen species (ROS) level

The level of intracellular ROS induced by Na₂SeO₃ was detected as described previously.⁵² In brief, after treatment with Na₂SeO₃ in different time, the MDCK cells were stained with DCFH-DA (10 μM) for 20 min. The level of ROS was detected by a fluorescence microscope. The fluorescence intensity was determined by a fluorescence plate reader with an excitation wavelength of 488 nm and emission wavelength of 525 nm respectively.

2.7 Western blotting analysis

The expression of proteins associated with different signaling pathways after treatment with Na₂SeO₃ in MDCK cells were analyzed by western blot as previously reported.⁵³ In brief, the four groups MDCK cells were lysed with RIPA solution after treatment with treatment for 48 h, followed by concentration detection of the proteins with a BCA kit. After that, equivalent amount of proteins were loaded in SDS-PAGE, then transferred to polyvinylidene difluoride membranes, and finally visualized by X-ray film.

2.8 Statistical analysis

All results were all obtained from three independent tests and presented as mean \pm S.D. The differences among multiple groups were compared using one-way analysis of variance (ANOVA). The probability of *P* value of <0.05 (*) and *P* value of <0.01 (**) were deemed to be statistically significant in all experiments.

3 Results and discussion

3.1 TCID₅₀ of H1N1

As shown in Table 1, the Reed-Muench assay was used to test the titer of H1N1 (TCID₅₀ = 107.7). H1N1 virus was used for *in vitro* study at the titer of 100 TCID₅₀.

Table 1 The Reed–Muench assay was used to test the titer of H1N1 (TCID₅₀ = 107.7)

Dilution of H1N1	Number of cells inoculated	Accumulation		Ratio of CPE
		CPE	No CPE	
10 ⁻¹	8	8	0	54
10 ⁻²	8	8	0	46
10 ⁻³	8	8	0	38
10 ⁻⁴	8	8	0	30
10 ⁻⁵	8	8	0	25
10 ⁻⁶	8	7	1	17
10 ⁻⁷	8	4	4	10
10 ⁻⁸	8	5	3	6
10 ⁻⁹	8	1	7	8
10 ⁻¹⁰	8	0	8	15
Blank	8	0	8	23
control	8	0	8	0

3.2 *In vitro* antiviral activity by Na₂SeO₃

The CCK-8 assay was performed to measure the anti-proliferation activity of H1N1 infected MDCK cells after treatment with Na₂SeO₃. As shown in Fig. 1A, the cell survival rate of cells which were treated with Na₂SeO₃ after infected by H1N1 (58.8%) was higher than cells without any treatment (26.4%), the resulted showed remarkably suppressed the viability of H1N1 and less cytotoxicity to normal cells (84.1%). As shown in Fig. 1B, after treatment with H1N1, the cell number decrease obviously, while cell survival rate in infected cells treated with Na₂SeO₃ was increased. These results indicated Na₂SeO₃ suppressed the infection of H1N1 effectively.

3.3 Inhibition of caspase-3 activation by Na₂SeO₃

Caspase-3 was confirmed as an important mediator of apoptosis in mammalian cells. As shown in Fig. 2, the treatment of MDCK

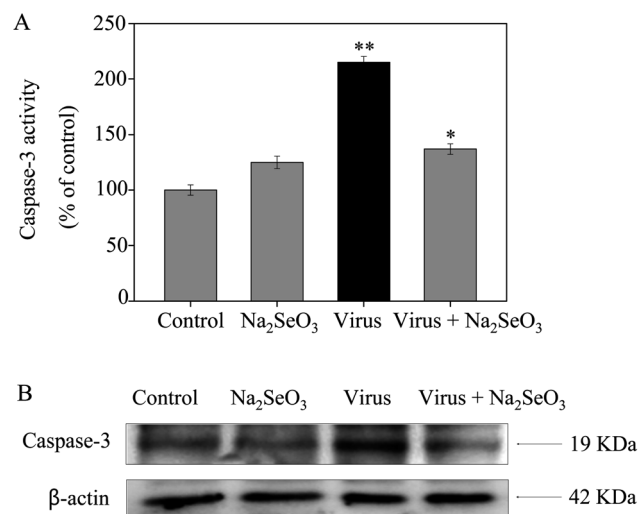


Fig. 2 Inhibition of caspase-3 activity by Na₂SeO₃. Cells were treated with Na₂SeO₃ and caspase-3 activity was detected by synthetic fluorogenic substrate. Concentration of Na₂SeO₃ was 1 μ M. Bars with different characters are statistically different at * $p < 0.05$ or ** $p < 0.01$ level.

cells with H1N1 influenza virus significantly increased the activity of caspase-3 (215%), but Na₂SeO₃ decreased the activity of caspase-3 (137%). These results show that Na₂SeO₃ inhibits H1N1 influenza virus activity through caspase-3 mediated apoptosis pathway.

3.4 Inhibition of ROS generation by Na₂SeO₃

The ROS generation was monitored by DCF fluorescence assay to indicate its role in the action mechanisms of Na₂SeO₃. As shown in Fig. 3A, the H1N1 influenza virus increased the

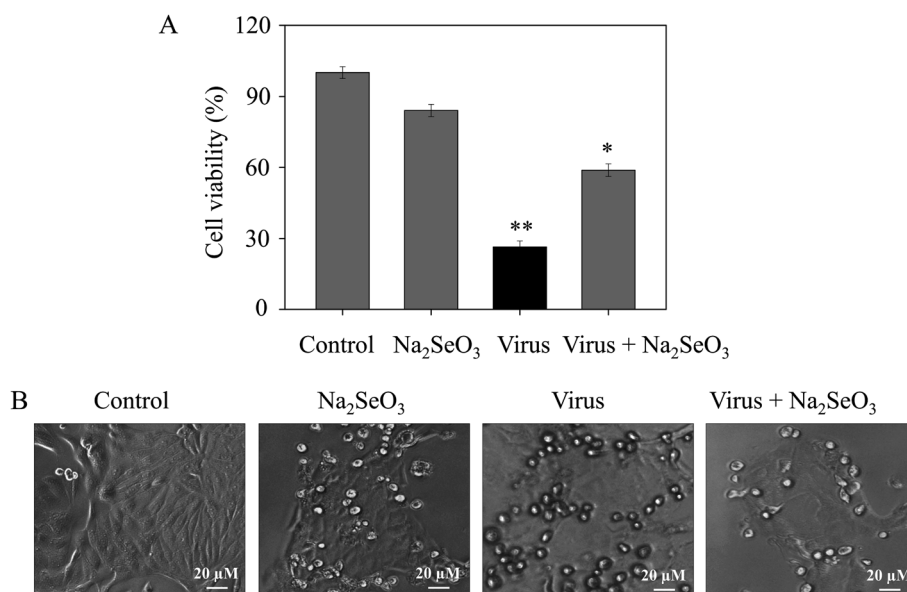


Fig. 1 Effects of Na₂SeO₃ on the growth of H1N1 infection of MDCK cells by CCK-8 assay. (A) Antiviral activity of Na₂SeO₃. Concentration of Na₂SeO₃ was 1 μ M. (B) Morphological changes in H1N1-infected MDCK cells observed by phase-contrast microscopy. Bars with different characters are statistically different at * $p < 0.05$ or ** $p < 0.01$ level.



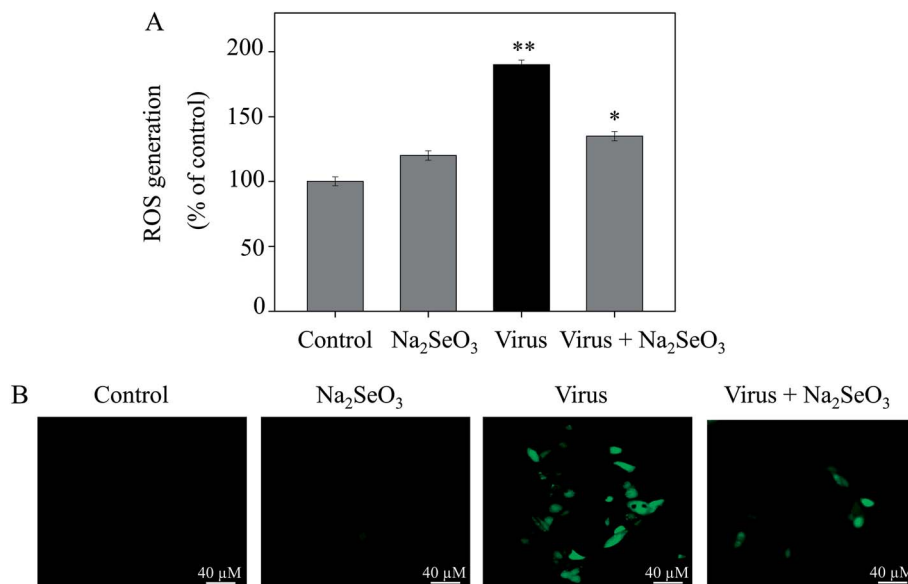


Fig. 3 ROS overproduction was inhibited by Na₂SeO₃ in H1N1 infection of MDCK cells (A) ROS levels were detected by DCF fluorescence intensity. (B) H1N1 infection of MDCK cells were preincubated with 10 μ M DCF for 30 min and then treated with Na₂SeO₃. Concentration of Na₂SeO₃ was 1 μ M. Bars with different characters are statistically different at * p < 0.05 or ** p < 0.01 level.

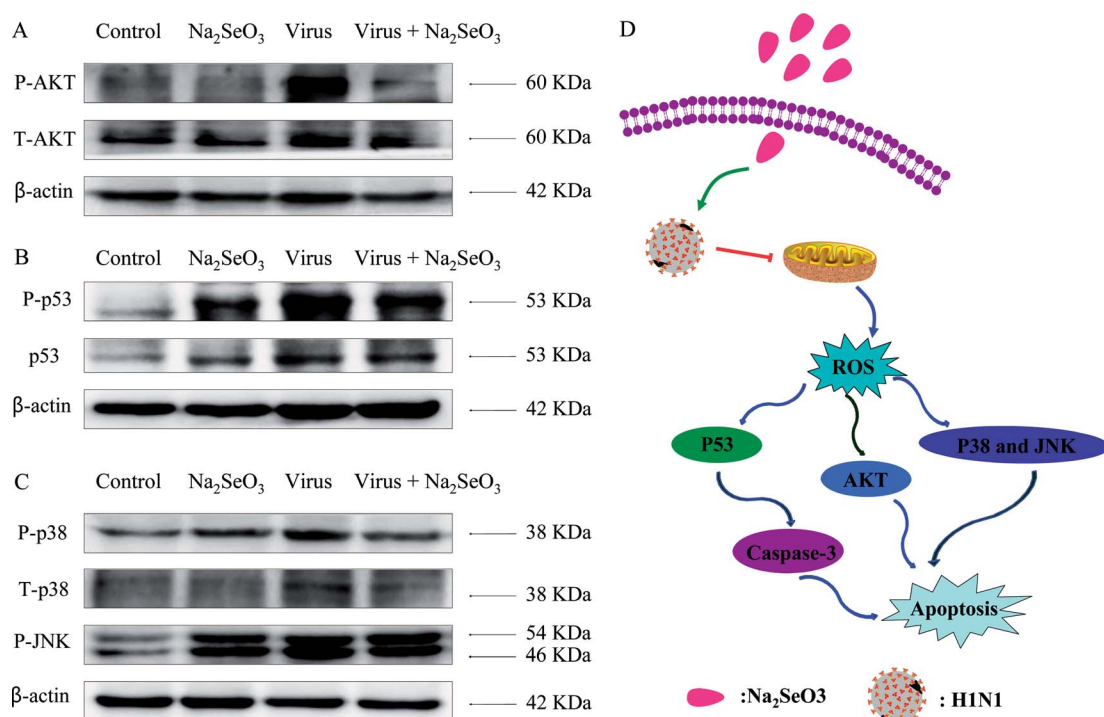


Fig. 4 Intracellular apoptotic signaling pathways by Na₂SeO₃ in H1N1 infection of MDCK cells. (A) Activation of AKT signaling pathway. (B) Phosphorylation status expression levels of p53 pathways. (C) Phosphorylation status expression levels of p38 and JNK pathways. (D) The main signaling pathway of ROS-mediated signaling pathways.

intracellular ROS generation in MDCK cells (190%). Na₂SeO₃ significantly decreased the intracellular ROS generation (135%). Stronger fluorescent intensity of DCF was found in MDCK cells by H1N1 influenza virus than Na₂SeO₃ as shown in Fig. 4B. These results indicated the involvement of ROS in the antiviral action of Na₂SeO₃.

3.5 ROS-mediated signaling pathways

The overexpression of ROS could lead to DNA damage and result in cell apoptosis through regulation of AKT and p53 signaling pathways. Due to the detection of ROS overproduction in cells exposed to H1N1 influenza virus, western blotting was

used to examine the effects on the ROS-mediated downstream pathways. As shown in Fig. 4A–C, treatments of the cells with Na_2SeO_3 obviously inhibited the expression levels of AKT, p53, p38 and JNK in MDCK cells. As showed in Fig. 4D, the results revealed that Na_2SeO_3 inhibited H1N1 influenza virus-induced MDCK cells apoptosis by ROS-mediated AKT and p53 and MAPK signaling pathways.

4 Conclusions

In conclusion, this study demonstrates that Na_2SeO_3 has the ability to inhibit the infection of H1N1 influenza virus *in vitro*. Na_2SeO_3 significantly reduced the population of apoptotic cells infected by H1N1 influenza virus. The potential molecular mechanisms have shown that the main mode by Na_2SeO_3 reduced cell death is apoptosis. The mechanism suggests that Na_2SeO_3 inhibits caspase-3 mediated apoptosis *via* ROS production. More importantly, studies of apoptotic signaling pathways triggered by Na_2SeO_3 in MDCK cells were the AKT, p53 and MAPK pathways. Therefore, our results indicate that Na_2SeO_3 has the ability to inhibit influenza virus in a safe dose range, and it can provide a selenium species for the development of antiviral drugs for influenza.

Author contributions

Yinghua Li and Guifang Gong designed the study, analyzed the experimental data and drafted the manuscript. Kunyan He and Qiumei Yang carried out the experiments. Min Guo, Tiantian Xu, Changbing Wang, Mingqi Zhao, Yi Chen, Miaomiao Du and Bingyuan Li participated in its design. Yanqing Huang and Bing Zhu refined the manuscript and coordination. All authors read and approved the final manuscript.

Conflicts of interest

The authors declare no competing financial interest.

Acknowledgements

This work was supported by the Technology Planning Project of Guangzhou (201804010183), the Medical Scientific Research Foundation of Guangdong Province (A2018306), the Pediatrics Institute Foundation of Guangzhou Women and Children's Medical Centre (YIP-2018-036 and YIP-2019-025), the Pediatrics Institute Foundation of Guangzhou Women and Children's Medical Centre (Pre-NSFC-2019-017 and IP-2018-004), the Guangdong Natural Science Foundation (2016A030313495), Science and Technology Plan Project of Guangdong Province (2014A020212602). Project of Traditional Chinese Medicine Bureau of Guangdong Province (20192075). The Guangzhou Medical University student's science and technology innovation project (2019AEK02).

Notes and references

- 1 A. Stevaert and L. Naesens, *Med. Res. Rev.*, 2016, **36**, 1127–1173.
- 2 S. J. Nabel GJ, *Nature*, 2019, **565**, 29–31.
- 3 A. D. Iuliano, K. M. Roguski, H. H. Chang, D. J. Muscatello, R. Palekar, S. Tempia, C. Cohen, J. M. Gran, D. Schanzer, B. J. Cowling, P. Wu, J. Kyncl, L. W. Ang, M. Park, M. Redlberger-Fritz, H. Yu, L. Espenhain, A. Krishnan, G. Emukule, L. van Asten, S. Pereira da Silva, S. Aungkulanon, U. Buchholz, M. A. Widdowson and J. S. Bresee, *Lancet*, 2018, **391**, 1285–1300.
- 4 C. Paules and K. Subbarao, *Lancet*, 2017, **390**, 697–708.
- 5 E. C. Hutchinson, *Trends Microbiol.*, 2018, **26**, 809–810.
- 6 Y. H. Li, Z. F. Lin, G. F. Gong, M. Guo, T. T. Xu, C. B. Wang, M. Q. Zhao, Y. Xia, Y. Tang, J. Y. Zhong, Y. Chen, L. Hua, Y. Q. Huang, F. L. Zeng and B. Zhu, *J. Mater. Chem. B*, 2019, **7**, 4252–4262.
- 7 R. G. Webster and E. A. Govorkova, *Ann. N. Y. Acad. Sci.*, 2014, **1323**, 115–139.
- 8 O. Suptawiwat, A. Kongchanagul, C. Boonarkart and P. Auewarakul, *Virus Res.*, 2018, **250**, 43–50.
- 9 K. S. Xue, L. H. Moncla, T. Bedford and J. D. Bloom, *Trends Microbiol.*, 2019, **26**, 781–793.
- 10 L. H. Moncla, N. W. Florek and T. C. Friedrich, *Trends Microbiol.*, 2017, **25**, 432–434.
- 11 V. N. Petrova and C. A. Russell, *Nat. Rev. Microbiol.*, 2018, **16**, 60.
- 12 F. Krammer, *Biotechnol. J.*, 2015, **10**, 690–U670.
- 13 K. Hoschler and M. C. Zambon, *Lancet*, 2017, **390**, 627–628.
- 14 D. M. Lyons and A. S. Lauring, *Viruses*, 2018, **10**, 407.
- 15 R. Nachbagauer and F. Krammer, *Clin. Microbiol. Infect.*, 2017, **23**, 222–228.
- 16 G. Dos Santos, E. Neumeier and R. Bekkati-Berkani, *Hum. Vaccines Immunother.*, 2016, **12**, 699–708.
- 17 K. S. Prabhu and X. G. Lei, *Adv. Nutr.*, 2016, **7**, 415–417.
- 18 M. Roman, P. Jitaru and C. Barbante, *Metallomics*, 2014, **6**, 25–54.
- 19 Q. Li, G. Y. Chen, W. Wang, W. J. Zhang, Y. Y. Ding, T. Zhao, F. Li, G. H. Mao, W. W. Feng, Q. Wang, L. Q. Yang and X. Y. Wu, *Int. J. Biol. Macromol.*, 2018, **117**, 878–889.
- 20 T. Zhang, G. Zhao, X. Y. Zhu, K. F. Jiang, H. C. Wu, G. Z. Deng and C. W. Qiu, *J. Cell. Physiol.*, 2019, **234**, 2511–2522.
- 21 G. F. Gong, B. L. Fu, C. X. Ying, Z. Q. Zhu, X. Q. He, Y. Y. Li, Z. X. Shen, Q. S. Xuan, Y. Q. Huang, Y. Lin and Y. H. Li, *RSC Adv.*, 2018, **8**, 39957–39966.
- 22 M. Guo, Y. H. Li, Z. F. Lin, M. Q. Zhao, M. S. Xiao, C. B. Wang, T. T. Xu, Y. Xia and B. Zhu, *RSC Adv.*, 2017, **7**, 52456–52464.
- 23 E. Mangiapane, A. Pessione and E. Pessione, *Curr. Protein Pept. Sci.*, 2014, **15**, 598–607.
- 24 M. Kieliszek, *Molecules*, 2019, **24**, 1298.
- 25 J. C. Avery and P. R. Hoffmann, *Nutrients*, 2018, **10**, 1203.
- 26 L. M. Watanabe, F. Barbosa, A. A. Jordao and A. M. Navarro, *Nutrition*, 2016, **32**, 1238–1242.
- 27 H. C. Anyabolu, E. A. Adejuyigbe and O. O. Adeodu, *AIDS Res. Treat.*, 2014, **2014**, 351043.



28 B. Shojadoost, R. R. Kulkarni, A. Yitbarek, A. Laursen, K. Taha-Abdelaziz, T. N. Alkie, N. Barjesteh, W. M. Quinteiro, T. K. Smith and S. Sharif, *Vet. Immunol. Immunopathol.*, 2019, **207**, 62–68.

29 K. Ivory, E. Prieto, C. Spinks, C. N. Armah, A. J. Goldson, J. R. Dainty and C. Nicoletti, *Clin. Nutr.*, 2017, **36**, 407–415.

30 D. L. Hatfield, P. A. Tsuji, B. A. Carlson and V. N. Gladyshev, *Trends Biochem. Sci.*, 2014, **39**, 112–120.

31 X. Y. Han, X. Y. Song, F. B. Yu and L. X. Chen, *Chem. Sci.*, 2017, **8**, 6991–7002.

32 M. Gao, R. Wang, F. B. Yu and L. X. Chen, *Biomaterials*, 2018, **160**, 1–14.

33 X. Zhang, Y. Huang, X. Y. Han, Y. Wang, L. W. Zhang and L. X. Chen, *Anal. Chem.*, 2019, **91**, 14728–14736.

34 Y. Huang, F. B. Yu, J. C. Wang and L. X. Chen, *Anal. Chem.*, 2016, **88**, 4122–4129.

35 X. Y. Song, X. Y. Han, F. B. Yu, X. Y. Zhang, L. X. Chen and C. J. Lv, *Theranostics*, 2018, **8**, 2217–2228.

36 K. Neha, M. R. Haider, A. Pathak and M. S. Yar, *Eur. J. Med. Chem.*, 2019, **178**, 687–704.

37 M. L. D. Leal, F. L. Pivot, G. C. Fausto, A. R. Aires, T. H. Grando, D. H. Roos, J. H. Sudati, C. Wagner, M. M. Costa, M. B. Molento and J. B. T. da Rocha, *Exp. Parasitol.*, 2014, **144**, 39–43.

38 C. W. Pyo, N. Shin, K. I. Jung, J. H. Choi and S. Y. Choi, *Biochem. Biophys. Res. Commun.*, 2014, **450**, 711–716.

39 K. M. Gowdy, Q. T. Krantz, C. King, E. Boykin, I. Jaspers, W. P. Linak and M. I. Gilmour, *Part. Fibre Toxicol.*, 2010, **7**, 34.

40 F. C. Camini, C. C. D. Caetano, L. T. Almeida and C. L. D. Magalhaes, *Arch. Virol.*, 2017, **162**, 907–917.

41 L. Liu, X. Tu, Y. F. Shen, W. C. Chen, B. Zhu and G. X. Wang, *Fish Shellfish Immunol.*, 2017, **67**, 211–217.

42 M. M. Liu, F. Z. Chen, T. Liu, F. M. Chen, S. W. Liu and J. Yang, *Microbes Infect.*, 2017, **19**, 580–586.

43 X. G. Xu, Y. Xu, Q. Zhang, F. Yang, Z. Yin, L. X. Wang and Q. F. Li, *Vet. Microbiol.*, 2019, **232**, 1–12.

44 T. S. Kang, W. Wang, H. J. Zhong, Z. Z. Dong, Q. Huang, S. W. Mok, C. H. Leung, V. K. Wong and D. L. Ma, *Cancer Lett.*, 2017, **396**, 76–84.

45 K. J. Wu, J. M. Huang, H. J. Zhong, Z. Z. Dong, K. Vellaisamy, J. J. Lu, X. P. Chen, P. Chiu, D. W. J. Kwong, Q. B. Han, D. L. Ma and C. H. Leung, *PLoS One*, 2017, **12**, 1–12.

46 K. J. Wu, H. J. Zhong, G. Yang, C. Wu, J. M. Huang, G. Li, D. L. Ma and C. H. Leung, *Chemistry*, 2018, **13**, 275–279.

47 X. Zi and A. R. Simoneau, *Cancer Res.*, 2005, **65**, 3479–3486.

48 Y. H. Hsin, C. F. Chen, S. Huang, T. S. Shih, P. S. Lai and P. J. Chueh, *Toxicol. Lett.*, 2008, **179**, 130–139.

49 R. Vlahos, J. Stambas and S. Selemidis, *Trends Pharmacol. Sci.*, 2012, **33**, 3–8.

50 Z. U. Rehman, C. C. Meng, Y. J. Sun, A. Safdar, R. H. Pasha, M. Munir and C. Ding, *Oxid. Med. Cell. Longevity*, 2018, 5123147.

51 Y. Li, Z. Lin, M. Zhao, T. Xu, C. Wang, L. Hua, H. Wang, H. Xia and B. Zhu, *ACS Appl. Mater. Interfaces*, 2016, **8**, 24385–24393.

52 Y. Li, Z. Lin, M. Guo, M. Zhao, Y. Xia, C. Wang, T. Xu and B. Zhu, *Int. J. Nanomed.*, 2018, **13**, 2005–2016.

53 Y. H. Li, Z. F. Lin, M. Q. Zhao, M. Guo, T. T. Xu, C. B. Wang, H. M. Xia and B. Zhu, *RSC Adv.*, 2016, **6**, 89679–89686.

